

## SOME ASPECTS OF SHALLOW WATER FLUCTUATIONS ON SAS PERFORMANCE

Nicholas G. Pace, ,  
Oddbjorn Bergem  
Marc Pinto

SACLANT Undersea Research Centre, La Spezia, Italy  
SACLANT Undersea Research Centre, La Spezia, Italy  
SACLANT Undersea Research Centre, La Spezia, Italy

### 1. INTRODUCTION

Small autonomous underwater vehicles (AUV), equipped with a high resolution sonar, have high potential for minehunting in very shallow water (VSW), 15 m water depth and below. Synthetic aperture sonar (SAS) techniques will allow this high resolution to be achieved with small transducers, compatible with the vehicle size. A SAS consists of a physical aperture which is translated in the medium by the AUV so as to form an extended virtual aperture [1]. Up to now, the research into SAS has focused chiefly on micronavigation [1], the measurement of the sonar trajectory during the SAS integration time with the sub-wavelength accuracy required for coherent processing. In addition to aided inertial navigation, micronavigation can be achieved using data-driven techniques, the most promising of which exploit the coherence properties of seafloor reverberation in conjunction with the displaced phase centre antenna technique (DPCA). [1]. As SAS technology is becoming more mature, it is becoming more important to investigate also the effect of non-benign environmental conditions to determine the SAS operation envelope. This paper investigates possible degradations on SAS performance due to effects induced by sea surface waves.

To form a SAS, multiple successive echoes from a potential target T are gathered by the AUV from distinct spatial locations  $A_1, A_2, \dots, A_N$  (Fig. 1). These are then delayed, to compensate for the two-way travel times from  $A_n$  to T, and then summed coherently. Of interest to SAS processing is those conditions under which medium fluctuations lead to random phase shifts  $\phi_1, \phi_2, \dots, \phi_N$  for each of the N travel times which may then destroy the coherent summation. The SAS performance can be quantified by the normalized expected gain of the SAS:

$$G = \frac{1}{N^2} \left\langle \left| \sum_{n=1}^N e^{j\phi_n} \right|^2 \right\rangle \quad \text{Equation 1}$$

Typically one requires  $10 \log G > -1$  dB to safely ignore the medium fluctuations

In this paper the effects of seasurface waves on the travel time of acoustic signals are investigated both theoretically and experimentally in the context of SAS systems.

### 2. SURFACE WAVE INFLUENCE ON ACOUSTIC SIGNALS

Phase fluctuations or travel time fluctuations caused by changes in the sound speed as a result of temperature, salinity and pressure may be termed a scalar effect. On the other hand the particle displacement velocity associated with the seasurface waves acts as a vector perturbation to the travel time. For one way transmission both scalar and vector effects will influence the signal, while a two-way transmission (backscattered) signal will be affected only by the scalar effect if it can be

assumed that the time scale associated with the variability is much longer than the two way travel time.

Here the relationship between the measured surface wave directional spectrum and the effective sound velocity are presented. The depth dependent horizontal particle displacement velocity associated with sea surface waves produces a vector addition to the mean sound speed. The depth dependent vertical particle displacement in the presence of vertical gradients in temperature and salinity produce a scalar addition to the mean sound velocity. These components together with a surface wave dependent pressure component are the essence of the model. The expression for the water surface elevation is [2]

$$\eta = \sum_n \left[ a_n \cos(k_n^1 x - \omega_n t + \phi_n) + \frac{1}{4} k_n a_n^2 \frac{(2 + \cosh(2k_n d)) \cosh(k_n d)}{\sinh^3(k_n d)} \cos(2(k_n^1 x - \omega_n t + \phi_n)) \right] \quad \text{Equation 2}$$

where the water depth is  $d$ ,  $x$  is the range,  $t$  is the time and  $a_n$  is a parameter which would simply be the amplitude of the  $n$ th spectral component if the second order term was absent.  $\phi_n$  is a uniformly distributed random starting phase for each spectral component. The relationship between the wavenumber  $k_n$  and the angular frequency  $\omega_n$  is

$$\omega_n^2 = g k_n \tanh(k_n d) = k_n^2 c_n^2 \quad \text{Equation 3}$$

$$\text{and } k_n^1 = k_n |\cos(\beta - \alpha_n)| \quad \text{Equation 4}$$

The mean direction of the  $n$ th spectral component is  $\alpha_n$  which is measured clockwise from the North. The mean square displacement of the water surface at any point may be written as

$$\langle \eta^2 \rangle = \sum_n S(f_n) \Delta f \quad \text{Equation 5}$$

where  $S(f_n)$  is the spectral density,  $2\pi f = \omega_n$  and  $\Delta f$  is the frequency interval.

The horizontal particle velocity of the water at a depth  $z$  below the water surface in a direction  $\beta$  measured clockwise from the North is given by  $u$  where  $z$  is negative downwards. [2]

$$u = \sum_n \left[ a_n \omega_n \frac{\cosh(k_n(z+d))}{\sinh(k_n d)} \cos(k_n^1 x - \omega_n t + \phi_n) + \frac{3}{4} (a_n k_n)^2 \times c_n \frac{\cosh(2k_n(z+d))}{\sinh^4(k_n d)} \cos(2(k_n^1 x - \omega_n t + \phi_n)) \right] \times \cos(\beta - \alpha_n) \quad \text{Equation 6}$$

Water surface elevation changes may give rise to a fluctuating sound speed at a given depth below the mean water surface due to pressure, temperature and salinity. The pressure changes are directly linked to the changes in water surface elevation. The temperature and salinity linked effects are due to vertical particle motion in the presence of vertical temperature and salinity gradients. The expression for the fluctuating pressure at depth  $z$  due to water surface elevation changes is [2]

Shallow water fluctuations and SAS performance – N G Pace, O Bergem & M Pinto

$$P = -\rho g z + \sum_n \left[ -\frac{\rho a_n^2 \omega_n^2}{4} \left( \frac{\cosh(2k_n(z+d))}{\sinh^2(k_n d)} \right) + \rho g a_n \frac{\cosh(k_n(z+d))}{\cosh(k_n d)} \cos(k_n^1 x - \omega_n t + \phi_n) \right. \\ \left. + \frac{\rho a_n^2 \omega_n^2}{4 \sinh^2(k_n d)} \left( \frac{3 \cosh(2k_n(z+d))}{\sinh^2(k_n d)} - 1 \right) \cos(2(k_n^1 x - \omega_n t + \phi_n)) \right]$$

Equation 7

The Mackenzie equation [3] for the sound speed requires depth, temperature and salinity.

$$c = 1448.96 + 4.591T - 5.304 \times 10^{-2} T^2 \\ + 2.374 \times 10^{-4} T^3 + 1.340(S - 35) \\ + 1.630 \times 10^{-2} z_p + 1.675 \times 10^{-7} z_p^2 \\ - 1.025 \times 10^{-2} T(S - 35) - 7.139 \times 10^{-13} T z_p^3$$

Equation 7

For this purpose the depth is taken as  $z_p$  where

$$z_p \rho g = P$$

Equation 8

and the temperature and salinity as

$$T = T_0 + \xi T_z$$

Equation 9

and

$$S = S_0 + \xi S_z$$

Equation 10

where  $T_0$  and  $S_0$  are the mean values of temperature and salinity at depth  $z$  and  $T_z$  and  $S_z$  are the vertical gradients. The vertical component of particle displacement is  $\xi$  where [2]

$$\xi = \sum_n \left[ a_n \frac{\sinh(k_n(z+d))}{\sinh(k_n d)} \cos(k_n^1 x - \omega_n t + \phi_n) \right. \\ \left. + \frac{3}{8} a_n^2 k_n \frac{\sinh(2k_n(z+d))}{\sinh^4(k_n d)} \cos(2(k_n^1 x - \omega_n t + \phi_n)) \right]$$

Equation 11

## 2.1 Phase Fluctuations

The effect of the sound speed fluctuations on the overall phase is obtained as follows. The travel time of an acoustic wave along a straight-line horizontal path of length  $x$  at depth  $z$  is

$$\tau(t) = \int_0^x \frac{dx}{c+u}$$

Equation 12

and the fluctuation is

$$\Delta\tau(t) = \tau(t) - \frac{x}{c_0} \quad \text{Equation 13}$$

where  $c_0$  is the mean sound speed at depth  $z$ . The phase fluctuation of the acoustic signal is

$$\Delta\Phi = 2\pi f_{\text{acoustic}} \Delta\tau \quad \text{Equation 14}$$

The model calculations presented here use the measured directional wave spectrum to provide the parameters  $a_n$

### 3. EXPERIMENT

Experimental measurements of the phase fluctuations in a shallow water site were obtained in April-June 1998. These have been described in some detail in previous publications [4], [5]. Essentially three transmitter towers and seven receive towers were placed in 10m of water as shown in Fig 1. Each transmitting tower had three omnidirectional transducers at 15kHz, 80kHz and 180kHz mounted on the top at a height of 4.5m from the seafloor. In front of each transmit tower a reception tower (R1, R2, R3) with a single hydrophone was placed. These hydrophones had two purposes: for the transducer closest to the hydrophone they acted as an acoustical reference while for the other two transmit towers they acted as a normal receiving hydrophone. In addition to these three receive towers, four other receive towers were placed on the leg between towers TX1 and TX2. Binary shift

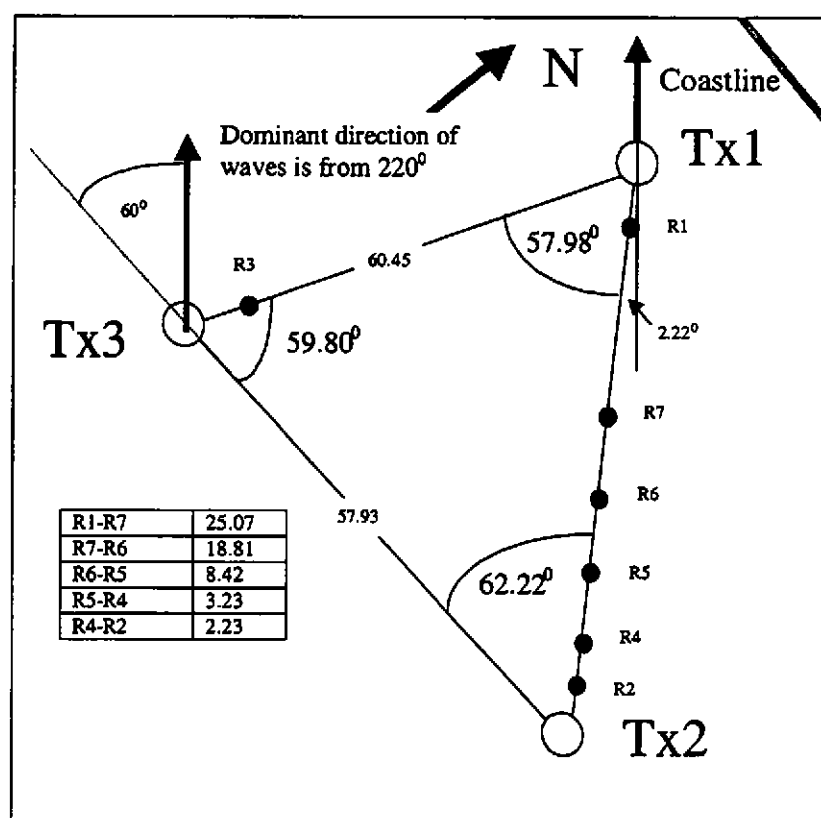


Figure 1 Geometry of the experiment

Shallow water fluctuations and SAS performance – N G Pace, O Bergem & M Pinto

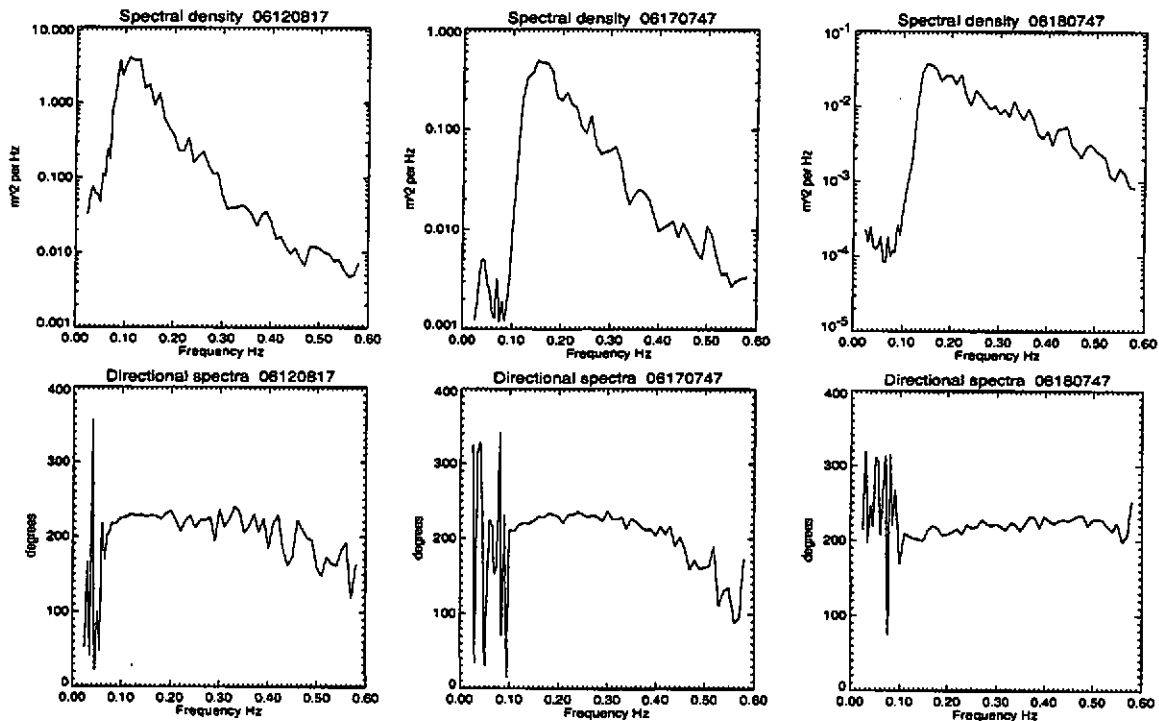


Figure 2 Wave spectra and their associated directional spectra for the 3 days., 12th, 17th and 18th June 1998 (from L to R)

coded signals were transmitted at the three carrier frequencies and a correlation technique used to extract the travel time to within a fraction of the acoustic wavelengths. Several environmental sensors were deployed close to the triangle. These included a directional waverider, CTD units, an acoustic doppler current profiler, a temperature chain and a weather station.

### 3.1 Experimental Data

In this paper attention is focussed on the phase fluctuations in the signals across the wavefronts of the transmissions from TX3 to receivers R1, R7, R6, R5, R4 and R2 during three periods in which the sea state was quite different. All data considered here are at 80kHz. The days concerned are the 12<sup>th</sup>, 17<sup>th</sup> and 18<sup>th</sup> June 1998. The spectral densities and their associated directional spectra are show in Figure 2. The direction of the waves containing most energy is from about 220 degrees during all three periods.

The directional wave rider provides  $S(f_n)$  and  $\alpha_n$  calculated from 20-minute segments. In order to use such data in the model the effective surface elevation parameter  $a_n$  is required. This may be calculated from

$$S(f_n) \Delta(f) = \frac{a_n^2}{2} + \frac{1}{2} \left( A_n \frac{k_n a_n^2}{4} \right)^2 \quad \text{Equation 15}$$

where

$$A_n = \frac{(2 + \cosh(2k_n d)) \cosh(k_n d)}{\sinh^3(k_n d)} \quad \text{Equation 16}$$

Shallow water fluctuations and SAS performance – N G Pace, O Bergem & M Pinto

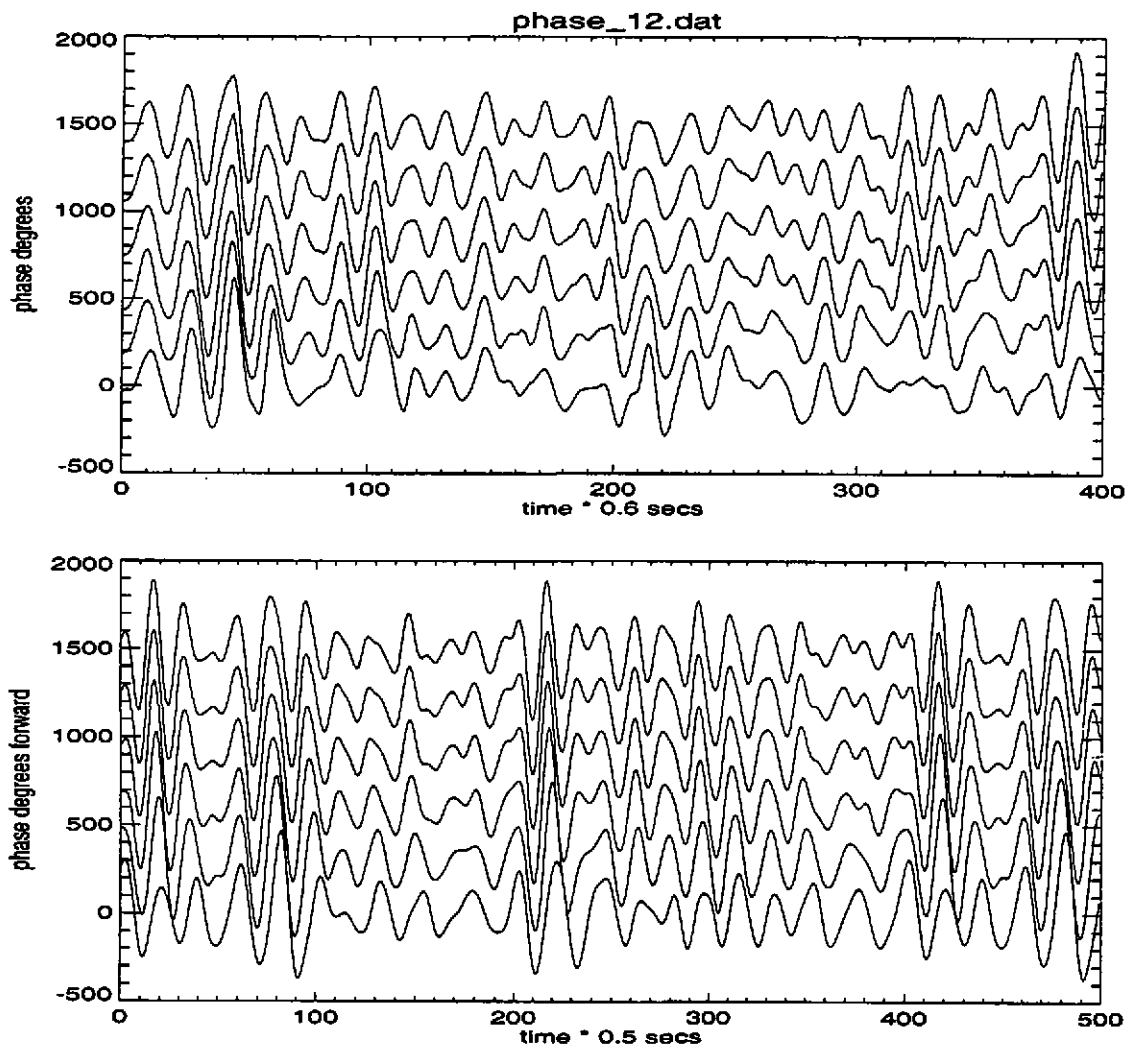


Figure 3 Transmission from TX3 to receivers R1, R7, R6, R5, R4, R2. ( R1 is the top trace).  
Upper: Experimental for day 12. Lower: Model

An example of the phase fluctuations seen on the receivers (R1, R7, R6, R5, R4 and R2) due to transmission from TX3 is shown in Figure 3 for a time period of about 250 seconds on day 12 together with the model output. It can be seen in Figure 4 that the contributions due to the scalar effects due to pressure and gradients in temperature and salinity are 'in phase' with the vector effects due to the particle displacement velocities. The phase fluctuations predicted by the forward transmissions of the model (TX3 to the receivers R1, R7, R6, R5, R4 and R2) are generally slightly higher than the experimental values. This could be adjusted by changes in the values taken for the temperature and salinity gradients,  $T_z$  and  $S_z$  respectively. Here, experimentally determined average values of 0.12 per sec and 0.15 ppt per m were used for the sound speed and salinity gradients respectively. In reference [5] some experimental results for reciprocal transmission paths were presented which showed the significant differences between reciprocal transmissions.

Shallow water fluctuations and SAS performance – N G Pace, O Bergem & M Pinto

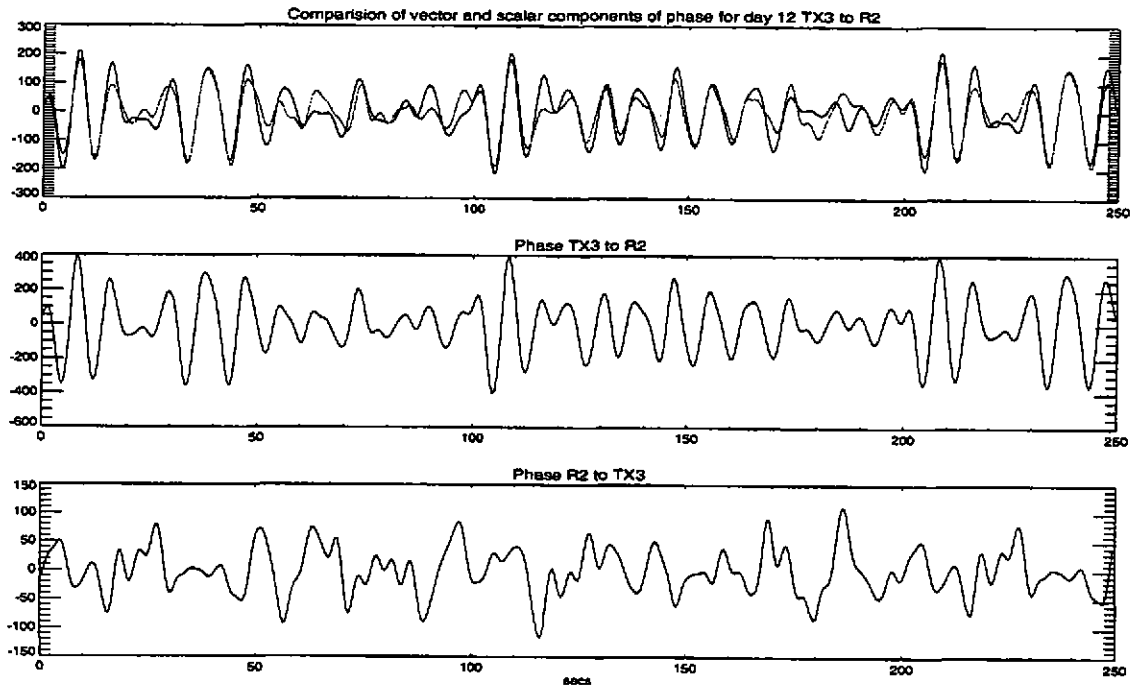


Figure 4 The modeled vector and scalar effects for transmission from TX3 to R2 is shown in top box. The middle and lower boxes show the modeled total phase fluctuations from TX3 to R2 and in the reverse direction.

3.2 Phase Gradients

The nature of the phase change at a given time across the receivers by R1, R7, R6, R5, R4 and R2 together with its evolution in time is of interest to the operation of SAS. Taking receiver R2 as a reference, it is found that for all three days the phase varies linearly with distance across the beam radiated from TX3. Figure 5 shows how the gradient of the linear fit varies with time.

The model results for the time evolution of the phase gradient and its standard deviation are similar to the experimental results

Day	Standard deviation degrees per m		
	Experiment	Model	
		Forward	Backward
12	2.5	3.9	2.0
17	0.41	0.85	0.24
18	0.14	0.18	0.15

Table 1 The standard deviation of the gradient of the linear fit to phase across the 60m aperture between R1 and R2 with TX3 as transmitter. Forward and backward refer to transmissions from Tx3 to R2.... and R2...toTx3 respectively.

Shallow water fluctuations and SAS performance – N G Pace, O Bergem & M Pinto

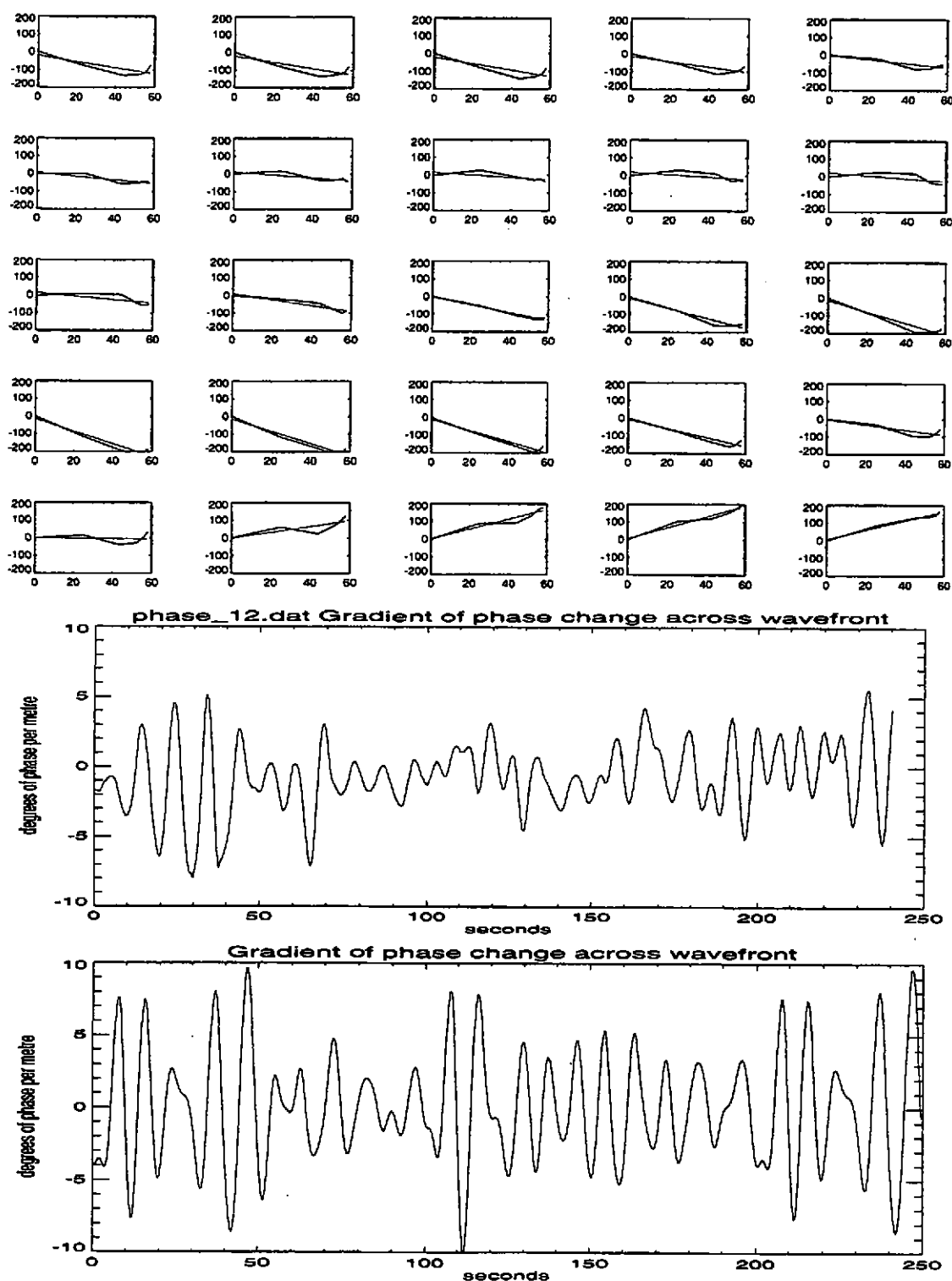


Figure 5 The linear fit to the phase across the 6 receivers is shown in the top box for the first 15 secs of the experimental data for day 12. The middle box shows the gradient of the linear fit as a function of time. The lower box shows the model calculations for the gradient.



Shallow water fluctuations and SAS performance – N G Pace, O Bergem & M Pinto

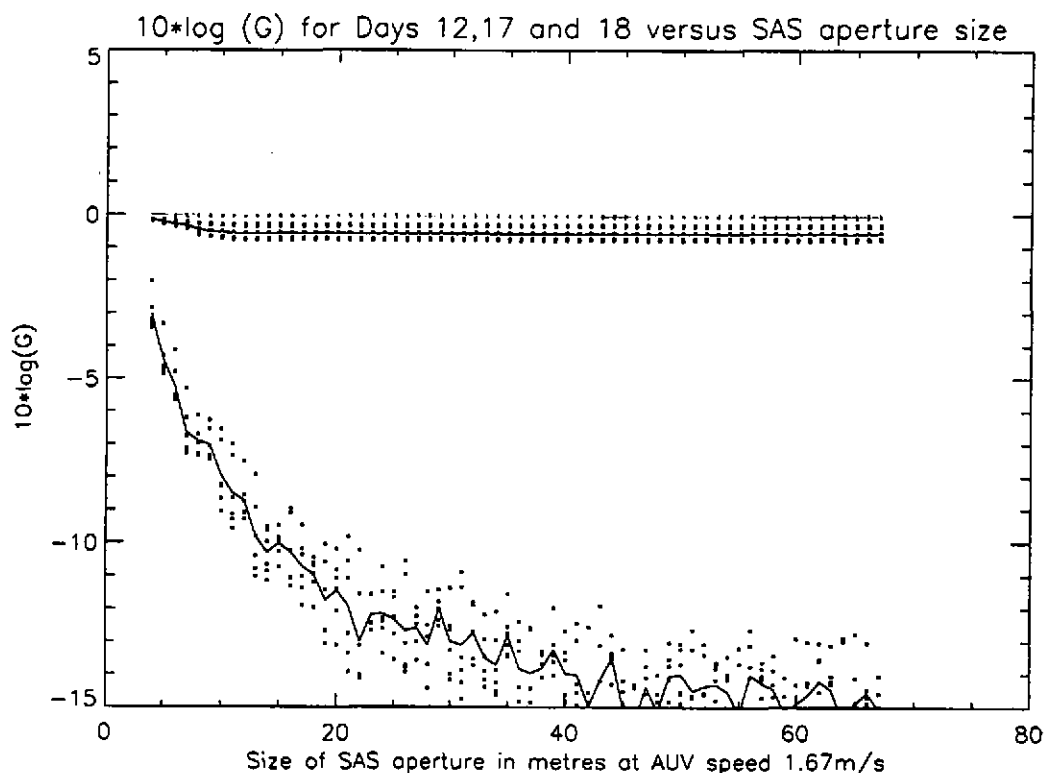


Figure 6 The G-parameter calculated from the data for the 6 receivers for conditions on the 3 days with the G parameter decreasing in the sequence day 18, 17, 12

#### 4. DISCUSSION

The experimental phase variation across the ~60 m aperture at a range of ~60m from the transmitter TX3 is approximately linear on all three days and has been reasonably well modeled. The temporal coherence function for the phase gradient is an oscillatory function and is driven by the sea surface wave spectrum. As the phase error across a physical receiving aperture is approximately linear, a target seen by this aperture would be in focus but misplaced in range and bearing by a small angular amount. For example at 80kHz a phase gradient of 5 degrees per metre causes an angular displacement of a target by 0.01 degrees.

The case of the SAS differs very much from that of the long physical aperture, in particular when the SAS integration time is larger than the temporal coherence time. Then two points in the synthetic aperture, distant spatially by more than the distance travelled by the AUV during this time, will suffer independent phase fluctuations which can then defocus the SAS. In Figure 6, the loss in SAS array gain is plotted as a function of SAS length and the sea state. This figure is encouraging, because it shows that the SAS operation envelope is probably quite large.

Futhermore, when DPCA is used to micronavigate the SAS, these medium fluctuations can be corrected for, provided the ping repetition period remains small compared to the temporal coherence time. The principle of DPCA is to effectively cancel the AUV displacement between two successive pings 1 and 2, so that identical echoes 1 and 2 will be received from the seafloor provided the medium and scatterer geometry is unchanged. It follows from above that the medium fluctuations will effectively displace the seafloor at ping 2 with respect to ping 1. This can be treated as an

Shallow water fluctuations and SAS performance – N G Pace, O Bergem & M Pinto

additional motion of the AUV between pings. For example, at a range of 60m, the angular displacement of 0.01 degrees discussed above corresponds to an apparent surge of an AUV of about 1cm between successive pings.

For sonar operations, a two-way transmission through the medium is required rather than the one-way case discussed above: transmission from the source to the target and then back to the receivers. For the monostatic case the vector part of the fluctuations will cancel for the outgoing and return paths but the scalar part, which as shown above can be substantial, will add for the two paths.

## 5. REFERENCES

- [1] Pinto, M.A. et al *Autofocussing a synthetic aperture sonar using the temporal and spatial coherence of seafloor reverberation*, In Pace, N.G. et al *High Frequency Acoustics in Shallow Water 1997* (SACLANTCEN CP-45) pp 417-432 ISBN 88-900194-1-7
- [2] B.J.Muga, J.F.Wilson. *Dynamic Analysis of Ocean structures*, Plenum 1970
- [3] K.V.Mackenzie, *Nine term equation for sound speed in the oceans*, J.Acoust.Soc.Amer. 70,807-812, 1981
- [4] O.Bergem, N.G.Pace, *Sound speed fluctuations and signal coherence in very shallow water: experimental description*. Proc Oceans98, 28sept-1 Oct 1998
- [5] O.Bergem, N.G.Pace, D.Di Iorio, *Surface wave influence on acoustic propagation in very shallow water*, Proc Oceans99, Sept 1999